Fermions coupled to skyrmions on S^3

2003 J. Phys. A: Math. Gen. 36 8141

(http://iopscience.iop.org/0305-4470/36/29/318)

INSTITUTE OF PHYSICS PUBLISHING JOURNAL OF PHYSICS A: MATHEMATICAL AND GENERAL

J. Phys. A: Math. Gen. **36** (2003) 8141–8163 PII: S0305-4470(03)63414-1

Fermions coupled to skyrmions on S^3

Steffen Krusch

Department of Pure Mathematics, School of Mathematics, University of Leeds, Leeds LS2 9JT, UK

E-mail: S.Krusch@maths.leeds.ac.uk

Received 13 May 2003
Published 8 July 2003
Online at stacks.iop.org/JPhysA/36/8141

Abstract

This paper discusses skyrmions on the 3-sphere coupled to fermions. The resulting Dirac equation commutes with a generalized angular momentum **G**. For $G = 0$ the Dirac equation can be solved explicitly for a constant Skyrme configuration and also for a $SO(4)$ symmetric hedgehog configuration. We discuss how the spectrum changes due to the presence of a non-trivial winding number, and also consider more general Skyrme configurations numerically.

PACS numbers: 03.50.Kk, 03.70.+k, 05.45.Yv, 11.10.Lm, 12.39.Dc

1. Introduction

The Skyrme model is a classical field theory which describes atomic nuclei and their low energy interactions [1]. It is a non-linear theory admitting topological solitons, so-called skyrmions, labelled by a topological charge B which can be identified with the baryon number. When the theory is quantized, the skyrmions give a good description of nuclei, Δ resonance [2] and even bound states of nuclei [3–5]. A striking feature is that skyrmions can be quantized as fermions [6, 7]. When the theory is coupled to a fermion field, two different ways of describing fermions appear in the same theory. Physically, the fermion field can be thought of as light quarks in the presence of atomic nuclei [8]. Hiller calculated the spectrum of the fermions in the background of a skyrmion [9]. However, the approximation for the skyrmion configuration was very crude. The spectrum shows a spectral flow of the eigenvalues depending on the value of the coupling constant. In particular one mode crosses zero. This general behaviour has been verified by other authors [10–12]. To gain a better understanding, we consider a generalization of the model. Since static field configurations in the original Skyrme model in flat space are topologically equivalent to maps $S^3 \to S^3$, the model can be generalized to the base space being a sphere of radius L. The original model is recovered in the limit $L \to \infty$. It turns out that for $L = 1$ and baryon number $B = 1$, the Faddeev–Bogomolny bound is satisfied and the minimal energy solution can be worked out explicitly [13]. In this case the map $S^3 \to S^3$ is an

isometry. For larger L the skyrmions are localized and tend to the usual flat space skyrmions in the limit $L \to \infty$.

Monopoles and skyrmions have many properties in common, and it is therefore instructive to recall the results for monopoles. There is an index theorem making use of the Bogomolny equations which states that for n monopoles there is a n dimensional vector space of fermionic zero modes [14]. Furthermore, the monopole and its fermionic zero mode can be calculated explicitly for $n = 1$. We will examine how far we can extend the analogy between monopoles and skyrmions.

In this paper we study fermions coupled to skyrmions on S^3. The Dirac equation on S^3 is derived in section 2. We also explain the skyrmion–fermion interaction. In section 3, we derive the ordinary differential equation which describes the solutions with total angular momentum $G = 0$ for general shape functions. In section 4.1, we give a brief discussion of ordinary differential equations and their regular singular points. In section 4.2, the equation of section 3 is solved for a constant Skyrme configuration, which is equivalent to a mass term for the fermions. We also discuss the boundary conditions which are necessary to derive the spectrum. In section 4.3, we derive the eigenfunctions and the spectrum for the hedgehog configuration with the special shape function $f(\mu) = \mu$. In section 5 the results of sections 4.2 and 4.3 are verified numerically. The spectrum for more general shape functions is also evaluated numerically and compared with results in the literature. We find an interesting relationship between the topological charge of the skyrmion and certain singular points. We end with a conclusion.

2. The Dirac equation on S^3

In this section we derive the Dirac equation on a 3-sphere of radius $L = 1$. First we define an atlas of two charts X_i and $\tilde{X}_i$ which are the stereographic projections from the north pole N and the south pole S, respectively. Next we define vierbeins on both charts which uniquely determine a connection 1-form using the metric compatibility condition and the torsion-free condition. The connection 1-form induces the spin connection so that we can finally write down the Dirac equation for each chart.[1] At the end of this section we discuss the interaction term which couples fermions and skyrmions.

In order to construct the stereographic projection, let S^3 be embedded in Euclidean $\mathbb{R}^4$ with coordinates (x_1, x_2, x_3, w). The points of S^3 can now be labelled by the projection from the north pole N onto the $\mathbb{R}^3$ plane through the equator introducing the coordinates X_i. Alternatively, one can project from the south pole S introducing the coordinates $\tilde{X}_i$. These two charts are well defined everywhere apart from their projection point N and S, respectively. In terms of the $\mathbb{R}^4$ Cartesian coordinates, we obtain

$$X_i = \frac{x_i}{1-w} \qquad \text{and} \qquad \tilde{X}_i = \frac{x_i}{1+w}. \tag{2.1}$$

In the following, we derive the equations of motion for both charts. As we shall see in section 4.2, this enables us to discuss the regularity conditions at the north and south poles in a simple way. We will also use the two charts to discuss a non-trivial symmetry of the energy spectrum in section 5.2.

The induced metric on S^3 can be calculated from the Euclidean metric in $\mathbb{R}^4$. Taking into account that our base space is a Lorentzian space time $\mathbb{R} \times S^3$, the metric can be written as

$$g = \operatorname{diag}\left(1, \frac{-4}{1+R^2}, \frac{-4}{1+R^2}, \frac{-4}{1+R^2}\right) \qquad \text{where} \quad R^2 = X_1^2 + X_2^2 + X_3^2. \tag{2.2}$$

[1] A good discussion of frame fields and spin connections can be found in [15], and also in [16].

The other coordinate system gives rise to the same metric replacing X_i by $\tilde{X}_i$. On the overlap, the two charts are related via the transition functions

$$\tilde{X}_i = \frac{1}{R^2} X_i. \tag{2.3}$$

Therefore, the coordinate vectors ∂_{X_i} and $\partial_{\tilde{X}_i}$ are related by

$$\partial_{\tilde{X}_i} = (R^2\delta_{ij} - 2X_iX_j)\partial_{X_j}. \tag{2.4}$$

Note that this transformation has the determinant $\det\left(\frac{\partial X_i}{\partial \tilde{X}_j}\right) = -R^6$. We now choose non-coordinate bases $\hat{e}_\alpha = e_\alpha{}^\mu \partial_{X_\mu}$ and $\hat{\tilde{e}}_\alpha = \tilde{e}_\alpha{}^\mu \partial_{\tilde{X}_\mu}$. It is convenient to choose diagonal vierbeins $e_\alpha{}^\mu$ and $\tilde{e}_\alpha{}^\mu$ such that

$$e_0{}^0 = 1 \quad \tilde{e}_0{}^0 = 1 \qquad e_i{}^i = -\frac{1+R^2}{2} \quad \tilde{e}_i{}^i = \frac{1+\tilde{R}^2}{2} \tag{2.5}$$

where all other components vanish. The minus sign occurs because X_i and $\tilde{X}_i$ are related by inversion which changes the orientation. The vierbeins satisfy

$$e_\alpha{}^\mu e_\beta{}^\nu g_{\mu\nu} = \eta_{\alpha\beta} \tag{2.6}$$

where $\eta_{\alpha\beta} = \mathrm{diag}(1,-1,-1,-1)$ is the flat Minkowski metric. The same relations are true for the vierbeins $\tilde{e}_\alpha{}^\mu$. The non-coordinate basis vectors are related by a $SO(3)$ transformation

$$\hat{\tilde{e}}_i = \frac{1}{R^2}(2X_iX_j - \delta_{ij})\hat{e}_j. \tag{2.7}$$

This is in fact a π rotation about the vector $\frac{X_i}{R}$. With this choice of vierbeins, the connection 1-form $\omega_{\alpha\beta}$ can be calculated from the metric compatibility condition $\omega_{\alpha\beta} = -\omega_{\beta\alpha}$ and the torsion-free condition

$$\mathrm{d}\hat{\theta}^\alpha + \omega^\alpha{}_\beta \wedge \hat{\theta}^\beta = 0 \tag{2.8}$$

where $\hat{\theta}^\alpha = e^\alpha{}_\mu \,\mathrm{d}X^\mu$ is the dual basis of $\hat{e}_\alpha$. After a short calculation, we obtain

$$\omega^{\alpha\beta} = \frac{2}{1+R^2}(X^\alpha \,\mathrm{d}X^\beta - X^\beta \,\mathrm{d}X^\alpha) \tag{2.9}$$

and the same relation holds for $\omega^{\alpha\beta}$ expressed in $\tilde{X}_i$ coordinates. The spin connection Ω_μ is now given by

$$\Omega_\mu \,\mathrm{d}X^\mu = -\frac{\mathrm{i}}{2}\omega^{\alpha\beta}\Sigma_{\alpha\beta} \tag{2.10}$$

where $\Sigma_{\alpha\beta} = \frac{\mathrm{i}}{4}[\gamma_\alpha, \gamma_\beta]$, and the γ matrices satisfy the standard anticommutation relations $\{\gamma_\alpha, \gamma_\beta\} = 2\eta_{\alpha\beta}$. The Lagrangian for fermions in curved space time is given by

$$\mathcal{L}_{\mathrm{fermion}} = \overline{\psi}\left(\mathrm{i}\gamma^\alpha e_\alpha{}^\kappa(\partial_\kappa + \Omega_\kappa)\right)\psi. \tag{2.11}$$

With our choice of coordinates and vierbeins, we obtain

$$\mathcal{L}_{\mathrm{fermion}} = \overline{\psi}(X_i,t)\left(\mathrm{i}\gamma^0\partial_t - \mathrm{i}\gamma^i\left(\frac{1+R^2}{2}\partial_{X_i} - X_i\right)\right)\psi(X_i,t) \tag{2.12}$$

using the coordinates X_i and

$$\mathcal{L}_{\mathrm{fermion}} = \overline{\tilde{\psi}}(\tilde{X}_i,t)\left(\mathrm{i}\gamma^0\partial_t + \mathrm{i}\gamma^i\left(\frac{1+\tilde{R}^2}{2}\partial_{\tilde{X}_i} - \tilde{X}_i\right)\right)\tilde{\psi}(\tilde{X}_i,t) \tag{2.13}$$

for the coordinates $\tilde{X}_i$. Equation (2.13) can be transformed into (2.12) by using $\tilde{X}_i = \frac{1}{R^2}X_i$ and the induced spinor transformation ρ of the fermion field $\psi(X_i,t)$ which we calculate in the following. The spinor transformation ρ is defined as

$$\tilde{\psi}(\tilde{X}_i) = \rho\psi(X_i). \tag{2.14}$$

The transformation ρ is a lifting of the local Lorentz transformation T of the vierbeins in (2.7). Note that the transformation $T_{ij} = (2\hat{X}_i\hat{X}_j - \delta_{ij})$ can be rewritten as

$$T(\alpha)_{ij} = \cos\alpha\,\delta_{ij} + \sin\alpha\,\epsilon_{ijk}\hat{X}_k + \hat{X}_i\hat{X}_j(1-\cos\alpha) \tag{2.15}$$

for $\alpha = \pi$. Here $\hat{X}_j = \frac{X_j}{R}$. Since we are only concerned with the spatial part, we work with the Euclidean δ_{ij} rather than with η_{ij}. Infinitesimally, the rotation is given by $T(\alpha)_{ij} = \delta_{ij} + \alpha\epsilon_{ijk}\hat{X}_k$. This can be lifted to a spinor transformation by $\rho(\alpha) = \exp\left(-\frac{\mathrm{i}}{2}\alpha\,\epsilon_{ijk}\hat{X}_k\Sigma_{ij}\right)$. For $\alpha = \pi$ we obtain

$$\rho = \mathrm{i}\gamma_0\gamma_5\gamma_j\hat{X}_j. \tag{2.16}$$

Note that there is a sign choice. As the spinor transformation ρ is an element of the double cover of the rotation group, the transformation $-\rho$ is also a lifting of the rotation T_{ij}.

In the following we discuss fermions coupled to skyrmions. The full Lagrangian $\mathcal{L}$ of this model is the sum of the fermion Lagrangian $\mathcal{L}_{\text{fermion}}$, the skyrmion Lagrangian $\mathcal{L}_{\text{skyrmion}}$ and the interaction Lagrangian $\mathcal{L}_{\text{int}}$. In this paper we consider fermions in the background of a static Skyrme configuration and neglect the backreaction. Therefore, we do not discuss the skyrmion Lagrangian any further, and the interested reader is referred to [17]. The interaction Lagrangian $\mathcal{L}_{\text{int}}$ given by

$$\mathcal{L}_{\text{int}} = -g\overline{\psi}(\sigma + \mathrm{i}\gamma_5\boldsymbol{\tau}\cdot\boldsymbol{\pi})\psi \tag{2.17}$$

where $U = \sigma + \mathrm{i}\boldsymbol{\tau}\cdot\boldsymbol{\pi}$ is a convenient parameterization of the Skyrme field. Equation (2.17) is the standard parity-invariant manner in which fermions couple to a Skyrme field and is also called the Yukawa interaction term. This Lagrangian was first introduced by Gell–Mann and Levy (without a fourth order Skyrme term), [18]. Also see [12] for a discussion of various different chiral models. Recently, the Lagrangian (2.17) has been discussed by Balachandran and Vaidya [8].

Note that ψ is a spin and an isospin spinor. In our notation the Pauli matrices $\boldsymbol{\tau}$ act on the isospin indices, whereas the γ matrices act on the spin indices. It is convenient to split the Dirac spinor into two 2×2 spin isospin matrices ψ_1 and ψ_2 such that

$$\psi = \begin{pmatrix}\psi_1\\ \psi_2\end{pmatrix}. \tag{2.18}$$

In this notation the γ matrices can be written in terms of quaternionic 2×2 matrices using i times the spin Pauli matrices $\boldsymbol{\sigma}$ and the two dimensional identity matrix I_2 as a basis for the quaternions. Since any complex 2×2 matrix can also be expressed in terms of quaternions with complex coefficients, it is convenient to choose the same basis for the quaternions as before. Then the spin isospin matrices ψ_i can be written as $\psi_i = a_0^{(i)}I_2 + \mathrm{i}a_k^{(i)}\sigma_k$. With this notation the spin operators act on ψ by left multiplication, $\sigma_k\psi_i$, whereas the isospin matrices act on ψ by right multiplication,

$$\tau_k\psi_i = \psi_i\sigma_k^T \tag{2.19}$$

$$= -\psi_i\sigma_2\sigma_k\sigma_2 \tag{2.20}$$

where the transpose in (2.19) guarantees the group structure, and (2.20) gives a useful trick to evaluate σ_i^T.

As mentioned above, we make the approximation that the skyrmion is a fixed static background field, i.e. we ignore the backreaction of the fermion fields. Furthermore, we only consider spherically symmetric skyrmions. For $B = 1$, skyrmions are believed to be spherically symmetric, but for $B > 1$ this is no longer true. However, we expect that some

generic features of the skyrmion–fermion interaction are not sensitive to the precise shape of the skyrmion. For more details see section 5.2. Spherically symmetric Skyrme fields are best written in polar coordinates

$$U = \exp(\mathrm{i} f(\mu)\mathbf{e}_\mu \cdot \boldsymbol{\tau}) \tag{2.21}$$

where $f(\mu)$ is the 'radial' shape function and $\mathbf{e}_\mu$ is the normal vector in μ direction, see (3.5). The shape function $f(\mu)$ can be calculated by solving the Euler–Lagrange equation of the Skyrme Lagrangian numerically. However, instead of using a numerical solution, it is more convenient in this context to approximate $f(\mu)$ by an explicit function. Manton showed in [19] that a good ansatz for L not too large is the conformal ansatz given by[2]

$$f(\mu) = 2\arctan\left(k\tan\frac{\mu}{2}\right). \tag{2.22}$$

Here k is a constant which has to be determined by minimizing the energy of the skyrmion. This ansatz describes a Skyrme configuration which is either localized around one of the poles or uniformly distributed. The value $k = 1$ corresponds to the $O(4)$ symmetric ansatz of the previous section, whereas for $k \ll 1$, or $k \gg 1$, the Skyrme field is localized at the south pole, or the north pole, respectively. Manton also showed that for $L \leqslant \sqrt{2}$, the stable solution is $k = 1$.

Finally, we can write down the Dirac equations for fermions coupled to a spherically symmetric background skyrmion. They are given by

$$\left(\mathrm{i}\gamma^0\partial_t - \mathrm{i}\gamma^i\left(\frac{1+R^2}{2}\partial_{X_i} - X_i\right) - gU^{\gamma_5}\right)\psi(X_i, t) = 0 \tag{2.23}$$

using the coordinates X_i and

$$\left(\mathrm{i}\gamma^0\partial_t + \mathrm{i}\gamma^i\left(\frac{1+\tilde{R}^2}{2}\partial_{\tilde{X}_i} - \tilde{X}_i\right) - gU^{\gamma_5}\right)\tilde{\psi}(\tilde{X}_i, t) = 0 \tag{2.24}$$

using the coordinates $\tilde{X}_i$. Here the skyrmion gives rise to

$$U^{\gamma_5} = \exp\left(\mathrm{i} f(\mu(R))\gamma_5\tau_i\frac{X_i}{R}\right) \tag{2.25}$$

and the same equation holds in the coordinate system $\tilde{X}_i$.

3. Solving the Dirac equation for $G = 0$

In order to solve the Dirac equation, we introduce spherical polar coordinates for equations (2.23) and (2.24). In terms of the coordinates $x = (x_1, x_2, x_3, w)$ in $\mathbb{R}^4$, the polar coordinates for the 3-sphere of radius 1 can be written as

$$x = (\sin\mu\sin\theta\cos\phi, \sin\mu\sin\theta\sin\phi, \sin\mu\cos\theta, \cos\mu)\,. \tag{3.1}$$

The angles (μ, θ, ϕ) can now be expressed in terms of X_i as

$$\begin{aligned}
\mu &= \begin{cases} \arctan\frac{2R}{R^2-1} + \pi & \text{for} \quad R^2 < 1 \\ \frac{\pi}{2} & \text{for} \quad R^2 = 1 \\ \arctan\frac{2R}{R^2-1} & \text{for} \quad R^2 > 1 \end{cases} \\
\theta &= \arctan\frac{\sqrt{X_1^2 + X_2^2}}{X_3} \\
\phi &= \arctan\frac{X_2}{X_1}.
\end{aligned} \tag{3.2}$$

[2] For $L \to \infty$ the ansatz tends to $f(r) = 2\arctan\frac{r}{r_0}$. Qualitatively, this is still a good ansatz.

In terms of the $\tilde{X}_i$, the relations for θ and ϕ are identical to those above, and for the μ coordinate we obtain

$$\mu = \begin{cases} \arctan \frac{2\tilde{R}}{1-\tilde{R}^2} & \text{for} \quad \tilde{R}^2 < 1 \\ \frac{\pi}{2} & \text{for} \quad R^2 = 1 \\ \arctan \frac{2\tilde{R}}{1-\tilde{R}^2} + \pi & \text{for} \quad \tilde{R}^2 > 1. \end{cases} \tag{3.3}$$

Equation (2.23) gives rise to the following Dirac equation in polar coordinates:

$$\left(\mathrm{i}\gamma^0 \partial_t + \mathrm{i}\gamma^i \left(e_{\mu i} \partial_\mu - \frac{e_{\theta i}\partial_\theta}{\sin\mu} - \frac{e_{\phi i}\partial_\phi}{\sin\mu \sin\theta} + \frac{e_{\mu i}\sin\mu}{1-\cos\mu} \right) - gU^{\gamma_5} \right) \psi = 0 \tag{3.4}$$

where $\psi = \psi(\mu, \theta, \phi, t)$ and the unit vectors $(e_\mu, e_\theta, e_\phi)$ are given by

$$e_\mu = \begin{pmatrix} \sin\theta\cos\phi \\ \sin\theta\sin\phi \\ \cos\theta \end{pmatrix} \qquad e_\theta = \begin{pmatrix} \cos\theta\cos\phi \\ \cos\theta\sin\phi \\ -\sin\theta \end{pmatrix} \qquad e_\phi = \begin{pmatrix} -\sin\phi \\ \cos\phi \\ 0 \end{pmatrix}. \tag{3.5}$$

U^{γ_5} can be written as $U^{\gamma_5} = \cos f(\mu) + \mathrm{i}\gamma_5 \mathbf{e}_\mu \cdot \boldsymbol{\tau} \sin f(\mu)$. Similarly, equation (2.24) gives rise to

$$\left(\mathrm{i}\gamma^0 \partial_t + \mathrm{i}\gamma^i \left(e_{\mu i} \partial_\mu + \frac{e_{\theta i}\partial_\theta}{\sin\mu} + \frac{e_{\phi i}\partial_\phi}{\sin\mu \sin\theta} - \frac{e_{\mu i}\sin\mu}{1+\cos\mu} \right) - gU^{\gamma_5} \right) \tilde{\psi} = 0. \tag{3.6}$$

The spin connection term could be removed by setting $\psi = \frac{1}{1-\cos\mu}\Phi$ and $\tilde{\psi} = \frac{1}{1+\cos\mu}\tilde{\Phi}$, respectively. However, it is easier to discuss the regularity of the solution in terms of the original fields.

We adopt the standard representation of the γ matrices where γ^0 is diagonal. This is convenient because the Dirac equation is invariant under parity,

$$\gamma^0 = \begin{pmatrix} I_2 & 0 \\ 0 & -I_2 \end{pmatrix} \qquad \gamma^i = \begin{pmatrix} 0 & \sigma_i \\ -\sigma_i & 0 \end{pmatrix} \qquad \gamma_5 = \begin{pmatrix} 0 & I_2 \\ I_2 & 0 \end{pmatrix}. \tag{3.7}$$

Now, the spinor transformation ρ in (2.16) can be evaluated explicitly:

$$\tilde{\psi}\left(\tilde{X}_i\right) = \begin{pmatrix} -\mathrm{i}\sigma_j \hat{X}_j & 0 \\ 0 & -\mathrm{i}\sigma_j \hat{X}_j \end{pmatrix} \psi\left(X_i\right). \tag{3.8}$$

With this choice of γ matrices, we can derive the differential equation for the stationary solutions of the Dirac equation by setting $\psi(X_i, t) = \mathrm{e}^{\mathrm{i}Et}\psi(X_i)$:

$$E\psi = \begin{pmatrix} g\cos f(\mu) & \boldsymbol{\sigma}\cdot\mathbf{p} + \mathrm{i}g\mathbf{e}_\mu \cdot \boldsymbol{\tau}\sin f(\mu) \\ \boldsymbol{\sigma}\cdot\mathbf{p} - \mathrm{i}g\mathbf{e}_\mu \cdot \boldsymbol{\tau}\sin f(\mu) & -g\cos f(\mu) \end{pmatrix} \psi \tag{3.9}$$

where

$$\boldsymbol{\sigma}\cdot\mathbf{p} = -\mathrm{i}\left(\mathbf{e}_\mu \cdot \boldsymbol{\sigma} \left(\partial_\mu + \frac{\sin\mu}{1-\cos\mu} \right) - \frac{1}{\sin\mu}\mathbf{e}_\theta \cdot \boldsymbol{\sigma}\partial_\theta - \frac{1}{\sin\mu\sin\theta}\mathbf{e}_\phi \cdot \boldsymbol{\sigma}\partial_\phi \right). \tag{3.10}$$

The components of the matrix in equation (3.9) commute with the total angular momentum operator $\mathbf{G} = \mathbf{L} + \mathbf{S} + \mathbf{I}$ where $\mathbf{L}$ is the orbital angular momentum operator, the spin operator is $\mathbf{S} = \frac{1}{2}\boldsymbol{\sigma}$ and the isospin operator is $\mathbf{I} = \frac{1}{2}\boldsymbol{\tau}$. In polar coordinates, the orbital angular momentum $\mathbf{L}$ is given by

$$\begin{aligned} L_x &= \mathrm{i}\left(\sin\phi\frac{\partial}{\partial\theta} + \cot\theta\cos\phi\frac{\partial}{\partial\phi} \right) \\ L_y &= \mathrm{i}\left(-\cos\phi\frac{\partial}{\partial\theta} + \cot\theta\sin\phi\frac{\partial}{\partial\phi} \right) \\ L_z &= -\mathrm{i}\frac{\partial}{\partial\phi}. \end{aligned} \tag{3.11}$$

Equation (3.9) is also invariant under parity $\hat{P}$ with

$$\hat{P}\psi(X_i) = \gamma_0\psi(-X_i) \quad \text{and} \quad \hat{P}X_i\hat{P}^{-1} = -X_i. \tag{3.12}$$

It is worth discussing the parity operator $\hat{P}$ in more detail. $\hat{P}$ acts on the γ matrices and the partial derivatives as follows:

$$\begin{aligned} &\hat{P}\gamma_0\hat{P}^{-1} = \gamma_0 \quad \text{and} \quad \hat{P}\gamma_i\hat{P}^{-1} = -\gamma_i \\ &\hat{P}\partial_0\hat{P}^{-1} = \partial_0 \quad \text{and} \quad \hat{P}\partial_i\hat{P}^{-1} = -\partial_i. \end{aligned} \tag{3.13}$$

Using the spinor transformation ρ in (2.16), we can show that

$$\hat{P}\tilde{\psi}(\tilde{X}_i) = -\gamma_0\tilde{\psi}(\tilde{X}_i). \tag{3.14}$$

Therefore, the parity operator $\hat{\tilde{P}}$ which is defined for the coordinates $\tilde{X}_i$ differs from $\hat{P}$ by a minus sign[3].

The $G^P = 0^+$ positive parity spin isospin spinors are given by

$$\psi(\mu,\theta,\phi) = \begin{pmatrix} (1-\cos\mu)^{\frac{1}{2}}G(\cos\mu)\sigma_2 \\ \mathrm{i}(1-\cos\mu)^{\frac{1}{2}}F(\cos\mu)(\mathbf{e}_\mu\cdot\boldsymbol{\sigma})\sigma_2 \end{pmatrix}. \tag{3.15}$$

This gives rise to the following system of first order differential equations:

$$\frac{\mathrm{d}}{\mathrm{d}\mu}\begin{pmatrix} F \\ G \end{pmatrix} = \begin{pmatrix} \frac{1-3\cos\mu}{2\sin\mu} - g\sin f & E - g\cos f \\ -(E+g\cos f) & g\sin f - \frac{3(1+\cos\mu)}{2\sin\mu} \end{pmatrix}\begin{pmatrix} F \\ G \end{pmatrix} \tag{3.16}$$

where F, G and f are functions of μ. Note that the $G^P = 0^-$ spinor

$$\psi(\mu,\theta,\phi) = \begin{pmatrix} \mathrm{i}(1-\cos\mu)^{\frac{1}{2}}F(\cos\mu)(\mathbf{e}_\mu\cdot\boldsymbol{\sigma})\sigma_2 \\ (1-\cos\mu)^{\frac{1}{2}}G(\cos\mu)\sigma_2 \end{pmatrix} \tag{3.17}$$

gives rise to the same equation with g replaced by $-g$.

In $\tilde{X}_i$ coordinates positive and negative parities are interchanged such that the 0^+ is given by

$$\tilde{\psi}(\mu,\theta,\phi) = \begin{pmatrix} \mathrm{i}(1+\cos\mu)^{\frac{1}{2}}\tilde{F}(\cos\mu)(\mathbf{e}_\mu\cdot\boldsymbol{\sigma})\sigma_2 \\ (1+\cos\mu)^{\frac{1}{2}}\tilde{G}(\cos\mu)\sigma_2 \end{pmatrix}. \tag{3.18}$$

This gives rise to

$$\frac{\mathrm{d}}{\mathrm{d}\mu}\begin{pmatrix} \tilde{F} \\ \tilde{G} \end{pmatrix} = \begin{pmatrix} -\frac{1+3\cos\mu}{2\sin\mu} + g\sin f & E + g\cos f \\ -(E - g\cos f) & \frac{3(1-\cos\mu)}{2\sin\mu} - g\sin f \end{pmatrix}\begin{pmatrix} \tilde{F} \\ \tilde{G} \end{pmatrix}. \tag{3.19}$$

Again the 0^- spinor

$$\tilde{\psi}(\mu,\theta,\phi) = \begin{pmatrix} (1+\cos\mu)^{\frac{1}{2}}\tilde{G}(\cos\mu)\sigma_2 \\ \mathrm{i}(1+\cos\mu)^{\frac{1}{2}}\tilde{F}(\cos\mu)(\mathbf{e}_\mu\cdot\boldsymbol{\sigma})\sigma_2 \end{pmatrix} \tag{3.20}$$

gives rise to the same equation with g replaced by $-g$.

Equation (3.16) can be transformed into a second order differential equation for $G(u)$ where $u = \cos\mu$. Note that since $\mu \in [0,\pi]$, it is consistent to set $\sin\mu = \sqrt{1-\cos^2\mu}$,

$$\begin{aligned} \Bigg((1-u^2)\frac{\mathrm{d}^2}{\mathrm{d}u^2} - \Bigg(4u + 1 + \frac{gf'\sin f\sqrt{1-u^2}}{E+g\cos f}\Bigg)\frac{\mathrm{d}}{\mathrm{d}u} + E^2 - g^2 - \frac{9}{4} + \frac{2g\sin f}{\sqrt{1-u^2}} \\ + \frac{3gf'\sin f}{2(E+g\cos f)}\frac{(1+u)}{\sqrt{1-u^2}} - \frac{g^2f'\sin^2 f}{E+g\cos f} - gf'\cos f\Bigg)G(u) = 0 \end{aligned} \tag{3.21}$$

[3] The origin of this sign difference is that the charts do not form an orientation atlas.

and similarly equation (3.19) can be transformed into

$$\left((1-u^2)\frac{\mathrm{d}^2}{\mathrm{d}u^2}-\left(4u-1-\frac{gf'\sin f\sqrt{1-u^2}}{E-g\cos f}\right)\frac{\mathrm{d}}{\mathrm{d}u}+E^2-g^2-\frac{9}{4}+\frac{2g\sin f}{\sqrt{1-u^2}}\right.$$
$$\left.+\frac{3gf'\sin f}{2(E-g\cos f)}\frac{(1-u)}{\sqrt{1-u^2}}-\frac{g^2f'\sin^2 f}{E-g\cos f}+gf'\cos f\right)\tilde{G}(u)=0. \tag{3.22}$$

It is not easy to transform equation (3.21) and (3.22) into each other. In fact, due to the spinor transformation (3.8) $\tilde{G}(u)$ and $F(u)$ are related via

$$F(u)=\sqrt{\frac{1+u}{1-u}}\tilde{G}(u). \tag{3.23}$$

Also note that $F(u)$ is given by

$$F(u)=\frac{1}{E+g\cos f}\left(\left(-\frac{3(1+u)}{2\sqrt{1-u^2}}+g\sin f\right)G(u)-\sqrt{1-u^2}\frac{\mathrm{d}}{\mathrm{d}u}G(u)\right) \tag{3.24}$$

and similarly $\tilde{F}(u)$ can be written as

$$\tilde{F}(u)=\frac{1}{E-g\cos f}\left(\left(\frac{3(1-u)}{2\sqrt{1-u^2}}-g\sin f\right)\tilde{G}(u)-\sqrt{1-u^2}\frac{\mathrm{d}}{\mathrm{d}u}\tilde{G}(u)\right). \tag{3.25}$$

4. Explicit solutions of the Dirac equation

In this section we solve the Dirac equation which has been derived in the previous section for various shape functions $f(\mu)$. However, first we review some basic facts about ordinary differential equations and regular singular points, following [20].

4.1. Differential equations and their singular points

Any linear second order differential equation can be brought into the standard form

$$y''(u)+P(u)y'(u)+Q(u)y(u)=0. \tag{4.1}$$

If $P(u)$ and $Q(u)$ are analytic functions in the neighbourhood of $u=u_0$, then $u=u_0$ is called a regular point. In this case there are locally two linearly independent solutions $y_1(u)$ and $y_2(u)$ such that any solution of (4.1) is a linear combination of $y_1(u)$ and $y_2(u)$. Moreover, $y(u)$ is an analytic function, i.e. it can be written as

$$y(u)=\sum_{n=0}^{\infty}a_n(u-u_0)^n. \tag{4.2}$$

If either $P(u_0)$ or $Q(u_0)$ is singular, then $u=u_0$ is called a singular point. In the special case that

$$P(u)=\frac{p(u)}{u-u_0} \tag{4.3}$$

$$Q(u)=\frac{q(u)}{(u-u_0)^2} \tag{4.4}$$

where $p(u)$ and $q(u)$ are analytic functions, i.e.

$$p(u)=p_0+p_1(u-u_0)+\cdots \quad \text{and} \quad q(u)=q_0+q_1(u-u_0)+\cdots \tag{4.5}$$

the point $u = u_0$ is called a *regular singular point*. Equations which only have regular or regular singular points are known as Fuchsian differential equations. Equation (4.1) can then be solved by the following ansatz:

$$y(u) = (u - u_0)^\rho \sum_{n=0}^{\infty} a_n (u - u_0)^n. \tag{4.6}$$

The exponent ρ can be calculated by solving the so-called *indicial equation*

$$\rho^2 + (p_0 - 1)\rho + q_0 = 0 \tag{4.7}$$

which is derived by inserting the ansatz (4.6) into (4.1). The two solutions (ρ_1, ρ_2) of the indicial equation (4.7) are called the *exponents* of the regular singular point u_0. Our convention will be that $\rho_1 \geqslant \rho_2$. If the difference of the exponents $s = \rho_1 - \rho_2$ is not a positive integer or zero, then the ansatz (4.6) gives rise to two linearly independent solutions of (4.1) which are uniformly convergent in some neighbourhood of u_0. Note, however, that the solution diverges at u_0 if its exponent ρ is negative.

Let $s = \rho_1 - \rho_2$ be a positive integer or zero. This situation is slightly more subtle because the two solutions can become linearly dependent, and this could lead to further logarithmic terms. The solution $y_1(u)$ with exponent ρ_1 is always uniformly convergent in some neighbourhood of u_0. Therefore, we reduce equation (4.1) to a differential equation of first order by setting $y(u) = y_1(u)z(u)$. This gives rise to the following equation for $z(u)$:

$$(u - u_0)^2 z''(u) + \left(2(u - u_0)^2 \frac{y_1'(u)}{y_1(u)} + (u - u_0)p(u) \right) z'(u) = 0. \tag{4.8}$$

This equation can be solved by integration and separation of variables, and we obtain

$$\begin{aligned} z(u) &= A + B_1 \int^u \frac{1}{(y_1(v))^2} \exp\left(- \int^v \frac{p(w)}{w - u_0}\, \mathrm{d}w \right) \mathrm{d}v \\ &= A + B_2 \int^u \frac{v - u_0}{(y_1(v))^2} \exp\left(-p_1(v - u_0) - \frac{1}{2} p_2 (v - u_0)^2 - \cdots \right) \mathrm{d}v \\ &= A + B_3 \int^u (v - u_0)^{-p_0 - 2\rho_1} g(v)\, \mathrm{d}v \end{aligned} \tag{4.9}$$

where $g(u)$ is an analytic function in a suitable domain, and A and B_i are constants. A short calculation shows that

$$-p_0 - 2\rho_1 = -s - 1. \tag{4.10}$$

Let

$$g(u) = 1 + \sum_{n=1}^{\infty} g_n (u - u_0)^n. \tag{4.11}$$

Then for $s \neq 0$ the most general solution is

$$y(u) = A y_1(u) + B(g_s y_1(u) \log(u - u_0) + \tilde{y}_2(u)) \tag{4.12}$$

where A and B are arbitrary constants, and $y_1(u)$ is the solution of the form (4.6). The constant g_s and the function $\tilde{y}_2(u)$ are completely determined by the differential equation (4.8). The function $\tilde{y}_2(u)$ is given by

$$\tilde{y}_2(u) = (u - u_0)^{\rho_2} \left(-\frac{1}{s} + \sum_{n=1}^{\infty} h_n (u - u_0)^n \right) \tag{4.13}$$

the coefficients h_n being constants. In the special case that $g_s = 0$, no logarithms occur, i.e. the two solutions $y_1(u)$ and $y_2(u)$ are linearly independent.

If $s = 0$ the corresponding form of the solution is

$$y(u) = Ay_1(u) + B\left(y_1(u)\log(u-u_0) + (u-u_0)^{\rho_2}\sum_{n=1}^{\infty} h_n(u-u_0)^n\right). \tag{4.14}$$

It is also possible to discuss the singularity at infinity. The transformation $v = \frac{1}{u}$ maps the point at infinity to the origin. If we apply this transformation to equation (4.1), we obtain a new differential equation in terms of v. If the new equation has a regular or a regular singular point at the origin $v = 0$, then (4.1) has a regular or regular singular point at infinity.

If a Fuchsian differential equation has n finite regular singular points $u = u_i$ with exponents $\rho_{1,2}^{(i)}$ and a regular singular point at infinity with exponents $\rho_{1,2}^{(\infty)}$, then the following equation holds:

$$\rho_1^{(\infty)} + \rho_2^{(\infty)} + \sum_{i=1}^{n}\left(\rho_1^{(i)} + \rho_2^{(i)}\right) = n - 1. \tag{4.15}$$

This is a useful consistency check for the exponents.

4.2. Fermions coupled to a constant Skyrme field

We are interested in the behaviour of fermions in the presence of a background skyrmion. The skyrmion introduces a space-dependent complex mass for the fermions. Therefore, it is instructive to consider first a massive fermion on S^3. This corresponds to $f(\mu) \equiv 0$ so that the fermion mass is g. This example can be solved explicitly in terms of hypergeometric functions. In the following sections we proceed to more complicated configurations. In section 4.3, we consider the spherically symmetric shape function $f(\mu) = \mu$ which can also be solved explicitly, but in a less standard way. In section 5.2, the conformal shape function (2.22) is discussed. In this case, the differential equation can no longer be solved explicitly. We present numerical algorithms in section 5.1.

Setting $f(\mu) = 0$, equation (3.21) can be written as

$$\left((1-u^2)\frac{\mathrm{d}^2}{\mathrm{d}u^2} - (4u+1)\frac{\mathrm{d}}{\mathrm{d}u} + e^2 - \frac{9}{4}\right)G(u) = 0 \tag{4.16}$$

where $e = \sqrt{E^2 - g^2}$.

Equation (4.16) has three regular singular points, one at $u = 1$, one at $u = -1$ and one at $u = \infty$ with exponents $\rho_{1,2}^{(1)} = \left(0, -\frac{3}{2}\right)$, $\rho_{1,2}^{(-1)} = \left(0, -\frac{1}{2}\right)$ and $\rho_{1,2}^{(\infty)} = \left(\frac{3}{2} + e, \frac{3}{2} - e\right)$ respectively. Note that relation (4.15) between the exponents is satisfied, i.e. the sum of the exponents is equal to 1. In this example we will show that the solution is non-singular on S^3 if its exponents are $\rho^{(-1)} = 0$ and $\rho^{(1)} = 0$.

Equation (4.16) can be solved explicitly:

$$G(u) = c_1\mathcal{F}\left(\tfrac{3}{2}+e, \tfrac{3}{2}-e; \tfrac{3}{2}; \tfrac{1}{2}(1+u)\right) + c_2(1+u)^{-\frac{1}{2}}\mathcal{F}\left(1+e, 1-e; \tfrac{1}{2}; \tfrac{1}{2}(1+u)\right) \tag{4.17}$$

where $\mathcal{F}(a, b; c; z)$ is a hypergeometric function, e.g. see [21, p 556]. The hypergeometric function is non-singular for $0 \leqslant z < 1$ and is normalized at $z = 0$, i.e. $\mathcal{F}(a, b; c; 0) = 1$. It may be singular at $z = 1$, corresponding to $u = 1$, which is the north pole. As $G(u)$ has to be non-singular at the south pole, $u = -1$, we have to set $c_2 = 0$.

Since $G(u)$ is not well defined at $u = 1$, we have to express $G(u)$ in terms of $\tilde{G}(u)$ and calculate $\tilde{G}(1)$. Using the transformation (3.8) from $\tilde{\psi}$ to ψ, we obtain

$$G(u) = \left(\frac{1+u}{1-u}\right)^{\frac{1}{2}} (-\mathrm{i}\sigma \cdot e_\mu \mathrm{i}\sigma \cdot e_\mu \tilde{F}(u))$$
$$= \left(\frac{1+u}{1-u}\right)^{\frac{1}{2}} \tilde{F}(u) \tag{4.18}$$

which is the analogue of equation (3.23). Setting $f(\mu) = 0$, in equation (3.22) we can derive a similar equation for $\tilde{G}(u)$ which has exponents $\rho_{1,2}^{(-1)} = \left(0, -\frac{3}{2}\right)$, $\rho_{1,2}^{(1)} = \left(0, -\frac{1}{2}\right)$ and $\rho_{1,2}^{(\infty)} = \left(\frac{3}{2}+e, \frac{3}{2}-e\right)$. The solution of this equation can again be expressed in terms of hypergeometric functions:

$$\tilde{G}(u) = \tilde{c}_1 \mathcal{F}\left(\tfrac{3}{2}+e, \tfrac{3}{2}-e; \tfrac{3}{2}; \tfrac{1}{2}(1-u)\right) + \tilde{c}_2 (1-u)^{-\frac{1}{2}} \mathcal{F}\left(1+e, 1-e; \tfrac{1}{2}; \tfrac{1}{2}(1-u)\right). \tag{4.19}$$

This is only non-singular at $u = 1$ if we set $\tilde{c}_2 = 0$. Assuming that $E - g \neq 0$, $\tilde{F}(u)$ can be calculated from equation (3.25):

$$\tilde{F}(u) = \frac{1}{E-g}\left(-\frac{3(1-u)}{2\sqrt{1-u^2}}\tilde{G}(u) + \sqrt{1-u^2}\frac{\mathrm{d}}{\mathrm{d}u}\tilde{G}(u)\right). \tag{4.20}$$

Therefore, $G(u)$ can be written as

$$G(u) = \frac{1}{E-g}\left((1+u)\frac{\mathrm{d}}{\mathrm{d}u}\tilde{G}(u) - \frac{3}{2}\tilde{G}(u)\right). \tag{4.21}$$

$\tilde{G}(u)$ has to be non-singular at $u = 1$. Equation (4.21) then implies that $G(u)$ is also non-singular at $u = 1$. Therefore, the regular solution $G(u)$ has the exponents $\rho^{(-1)} = 0$ and $\rho^{(1)} = 0$. Note that this argument only relies on the local behaviour, and explicit solutions are not needed. As we shall see, in the generic case, the exponents at the singular points do not depend on the chosen shape function, so that our analysis is also valid for general shape functions. Problems can occur if additional singular points coalesce with the singular points at $u = \pm 1$ because this changes the exponents[4]. In the generic case, the regular solution can be calculated by imposing that the solution can be expanded as a power series at the north and at the south pole. Later, this will be the basis for our numerical algorithm. Now, we impose this condition in order to calculate the spectrum of equation (4.16).

Using formula (15.3.6) in [21] we can express $G(u)$ in terms of hypergeometric functions at the second singular point[5],

$$G(u) = c_1 \mathcal{F}\left(\frac{3}{2}+e, \frac{3}{2}-e; \frac{3}{2}; \frac{1}{2}(1+u)\right)$$
$$= c_1 \left(\frac{\Gamma\left(\frac{3}{2}\right)\Gamma\left(-\frac{3}{2}\right)}{\Gamma(e)\Gamma(-e)}\mathcal{F}\left(\frac{3}{2}+e, \frac{3}{2}-e; \frac{5}{2}; \frac{1}{2}(1-u)\right)\right. \tag{4.22}$$
$$\left. + \left(\frac{1-u}{2}\right)^{-\frac{3}{2}} \frac{\Gamma\left(\frac{3}{2}\right)\Gamma\left(\frac{3}{2}\right)}{\Gamma\left(\frac{3}{2}-e\right)\Gamma\left(\frac{3}{2}+e\right)}\mathcal{F}\left(-e, e; -\frac{1}{2}; \frac{1}{2}(1-u)\right)\right).$$

The last term has to vanish, otherwise $\tilde{F}(u)$ would be singular at the north pole. Therefore, either $\Gamma\left(\frac{3}{2}+e\right)$ or $\Gamma\left(\frac{3}{2}-e\right)$ has to have a pole. Since $e \geqslant 0$, we obtain $e = N + \frac{3}{2}$, and the spectrum is therefore

$$E = \pm\sqrt{g^2 + \left(N+\tfrac{3}{2}\right)^2} \qquad \text{where} \quad N = 0, 1, 2, \ldots. \tag{4.23}$$

[4] In the following section we will also discuss the case that further singular points are inside the interval $(-1, 1)$.

[5] Equation (4.22) only holds if $|\arg(1-z)| < \pi$. However, this inequality is satisfied because $(1-z) = \frac{1}{2}(1+\cos\mu) \geqslant 0$.

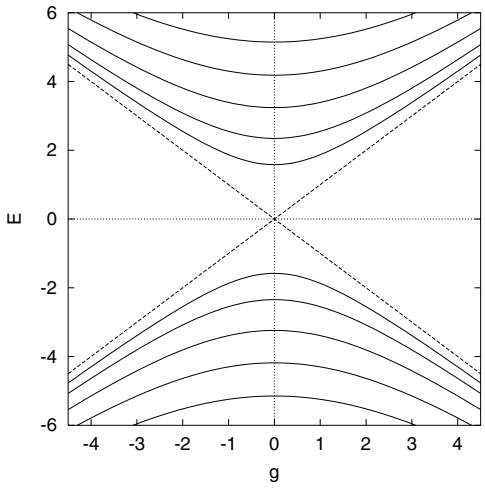

Figure 1. The energy levels E_n as a function of the coupling constant g for $f(\mu) = 0$. $E = \pm g$ is shown as dashed lines.

With this condition the eigenfunctions $G_N(u)$ reduce to Jacobi polynomials ([21], formula 15.4.6).

The spectrum is displayed in figure 1. It is symmetric with respect to $E = 0$. The importance of this result lies in the fact that for $g = 0$ the energy E_N and the corresponding solutions $G_N(u)$ are the same for all possible shape functions $f(\mu)$. Therefore, these solutions can be used as starting values for the relaxation method, which will be described in section 5. As the radius of the 3-sphere tends to infinity, the spectrum tends to the usual spectrum of the Dirac equation, which is continuous for $E^2 \geqslant g^2$. Also note that if we assume that $G(u)$ and its first and second derivatives remain finite as g tends to infinity, then the energy E has to be of order g in this limit, so $\pm g$ is the leading order asymptotic for E. Therefore, we displayed the lines $E = \pm g$ in figure 1. As we shall see in section 5 the region $E^2 < g^2$ also plays a special role for our numerical algorithm.

Another way of deriving the spectrum (4.23) is to note that if the exponents at $u = \pm 1$ both vanish, then $G(u)$ is an integral function, that is it has only one singular point at infinity. The only integral functions which do not possess an essential singular point at infinity are the polynomials, e.g. [20, p 106]. Therefore, one of the exponents at infinity is equal to $-N$ for $N = 0, 1, \ldots$. Since the exponents at infinity are $\rho_{1,2}^{(\infty)} = \left(e + \frac{3}{2}, -e + \frac{3}{2}\right)$, we obtain the same spectrum as before. Note, however, that since the exponents $\rho_{1,2}^{(\infty)}$ differ by an integer, we have to check in this approach that the solution is indeed a polynomial, i.e. g_s in equation (4.11) vanishes. This spectrum has also been calculated by other authors, e.g. [22, 23].

4.3. Fermions coupled to the Skyrme field $f(\mu) = \mu$

In this section we construct the solutions of equation (3.21) for $f(\mu) = \mu$. Configurations with $f(\mu) \neq 0$ are called 'hedgehog configurations' because at each point the vector in isospin space is proportional to the coordinate vector. For $f(\mu) = \mu$ the map from the base S^3 to the target S^3 is even an isometry and possesses $O(4)$ symmetry. Setting $f(\mu) = \mu$ in

equation (3.21), we obtain

$$(1-u^2)(E+gu)\frac{\mathrm{d}^2G}{\mathrm{d}u^2} - ((4u+1)(E+gu)+g(1-u^2))\frac{\mathrm{d}G}{\mathrm{d}u} + \left((E+gu)\left(E^2-g^2+2g-\frac{9}{4}-gu\right)+\frac{3}{2}g(1+u)-g^2(1-u^2)\right)G=0. \tag{4.24}$$

This is a homogeneous differential equation of Fuchsian type with four singular points. They are located at $u=\pm1$, $u=-\frac{E}{g}$ and $u=\infty$. Assuming $E\neq\pm g$ the exponents are

$$\begin{aligned}\rho_{1,2}^{(1)} &= \left(0,-\tfrac{1}{2}\right)\\ \rho_{1,2}^{(-1)} &= \left(0,-\tfrac{3}{2}\right)\\ \rho_{1,2}^{(-\frac{E}{g})} &= (2,0)\\ \rho_{1,2}^{(\infty)} &= \left(1\pm\tfrac{1}{2}\sqrt{1-4E+4E^2+8g-4g^2}\right).\end{aligned} \tag{4.25}$$

For $E=g$ the singular points at $u=-1$ and $u=-\frac{E}{g}$ coalesce, and therefore, the exponents at $u=-1$ become $\rho_{1,2}^{(-1)}=\left(\frac{1}{2},0\right)$ and the exponent at infinity is $\rho_{1,2}^{(\infty)}=\left(1\pm\frac{1}{2}\sqrt{1+4g}\right)$. The relation for the exponents (4.15) is satisfied. For $E=-g$ the singular points at $u=1$ and $u=-\frac{E}{g}$ coalesce. This changes the exponents at $u=1$ to $\rho_{1,2}^{(1)}=\left(-1,-\frac{3}{2}\right)$. In this case, there is an essential singular point at infinity and the equation is no longer Fuchsian.

Since we are interested in solutions that can be expanded as a power series around $u=\pm1$, it is natural to look for polynomial solutions. The singular point at $u=-\frac{E}{g}$ might impose a constraint. In order to verify whether there is a logarithmic term, we have to calculate the coefficient g_s in equation (4.11). Here $s=2$. After a standard calculation, we obtain $g_2=0$. Therefore, there are two independent power series at the point $u=-\frac{E}{g}$. This imposes no further restriction, since we do not have to exclude any of these two solutions. This implies that $G(u)$ is again an integral function and we can calculate the energy spectrum using the exponents at infinity. Again, the exponents $\rho_{1,2}^{(\infty)}$ differ by an integer, and we have to verify that the solutions are indeed polynomials. It turns out that the only problem occurs for $\rho_2^{(\infty)}=0$.

In the following, we derive the recurrence relation for these polynomials. Yet, it is instructive to consider first the solution where $G(u)$ is a constant a_0, i.e. $\rho_2^{(\infty)}=0$. Then we can solve equation (4.25) for E and obtain $E=g-\frac{1}{2}$ and $E=\frac{3}{2}-g$. Setting $G(u)=a_0$ in equation (4.24), we obtain

$$\left(E+g-\tfrac{3}{2}\right)\left(g\left(E-g+\tfrac{1}{2}\right)(u+1)+\left(E-g+\tfrac{3}{2}\right)(E-g)\right)a_0=0. \tag{4.26}$$

It is easy to see that this is not a solution for $E=g-\frac{1}{2}$. $G(u)=a_0$ is only a solution for arbitrary g if $E=\frac{3}{2}-g$. This solution is very interesting because its spectrum crosses $E=0$ for $g=\frac{3}{2}$.

Now we derive the general solution for equation (4.24). Since we are interested in the solutions for which the relevant exponent vanishes for $u=-1$, we expand $G(u)$ around the south pole $u=-1$:

$$G(u)=\sum_{n=0}^{\infty}a_n(u+1)^n. \tag{4.27}$$

Assuming that $E\neq g$, we derive the following recurrence relations. The initial condition is

$$a_1=-\tfrac{1}{3}\left(E^2-\left(g-\tfrac{3}{2}\right)^2\right)a_0 \tag{4.28}$$

and the recurrence relation is given by

$$a_{n+1} = \frac{\left((E-3g)n^2 + (3E-2g)n - (E-g)\left(E^2 - \left(g-\frac{3}{2}\right)^2\right)\right)}{(E-g)(2n+3)(n+1)} a_n + \frac{g\left(n^2 - \left(E^2 - E - g^2 + 2g + \frac{1}{4}\right)\right)}{(E-g)(2n+3)(n+1)} a_{n-1}. \tag{4.29}$$

Since we have an initial condition, we expect to be able to reduce this second order recurrence relation to a recurrence of first order. Therefore, we make the ansatz

$$a_n = \prod_{i=0}^{n-1} b_i. \tag{4.30}$$

Substituting this ansatz into the recurrence relation (4.29), we obtain a non-linear first order recurrence for b_n. However, this can be solved by setting

$$b_n = -\frac{(2E-2g+1+2(n+1))\left(E^2 - E + 2g - g^2 + \frac{1}{4} - (n+1)^2\right)}{(2E-2g+1+2n)(2n+3)(n+1)}. \tag{4.31}$$

By construction, the series (4.27) has the right behaviour at the singular point $u = -1$. To find the behaviour at $u = 1$, we have to discuss the radius of convergence R_{conv} of the series. The radius R_{conv} can be calculated as the following limit:

$$\begin{aligned} R_{\text{conv}} &= \lim_{n\to\infty} \left|\frac{a_n}{a_{n+1}}\right| \\ &= \lim_{n\to\infty} \frac{1}{|b_n|} \\ &= 2. \end{aligned} \tag{4.32}$$

Therefore, the series converges for $u \in [-1, 1)$. For $u = 1$, equation (4.27) can be written as

$$G(1) = \sum_{n=0}^{\infty} a_n 2^n. \tag{4.33}$$

For large n, b_n behaves like $\frac{1}{2}$. Therefore, a_n is proportional to $\left(\frac{1}{2}\right)^n$ so that the terms in the sum (4.33) are of order 1 and do not vanish. Hence, the series is divergent, unless it terminates. But because of the special form of a_n and b_n, it is easy to see when the series terminates. In fact, for $n > 0$ we can now write a_n as the following product:

$$a_n = \frac{\left(E+g-\frac{3}{2}\right)\left(E+g-\frac{n}{2}\right)}{n!(2n+1)!!} \prod_{i=1}^{n} \left(E^2 - E + 2g - g^2 + \frac{1}{4} - (\mathrm{i}+1)^2\right) \tag{4.34}$$

where $(2n+1)!!$ is the product of all odd numbers less than or equal to $(2n+1)$. All a_n vanish for $E = \frac{3}{2} - g$ which is the constant solution that we have derived previously. If the term $\left(E+g-\frac{n}{2}\right)$ vanishes, then the coefficient for a_n vanishes individually. However, if one of the terms in the product vanishes, say for $n = N_0$, then not only a_{N_0} vanishes but also all a_N for $N \geqslant N_0$, i.e. the series terminates.

From this condition the complete energy spectrum can be calculated. We obtain the special level $E_0 = \frac{3}{2} - g$ which crosses from positive to negative energies, and two series of energy levels E_n^+ and E_n^- which are given by

$$E_n^{\pm} = \tfrac{1}{2} \pm \sqrt{n^2 + 2n + (g-1)^2} \qquad \text{for} \quad n = 1, 2, \ldots. \tag{4.35}$$

The spectrum is displayed in figure 2. If we only consider the modes with energy $E_n^{\pm}$ the spectrum is symmetric under reflection at the axes $g = 1$ and $E = \frac{1}{2}$. However, the mode 0

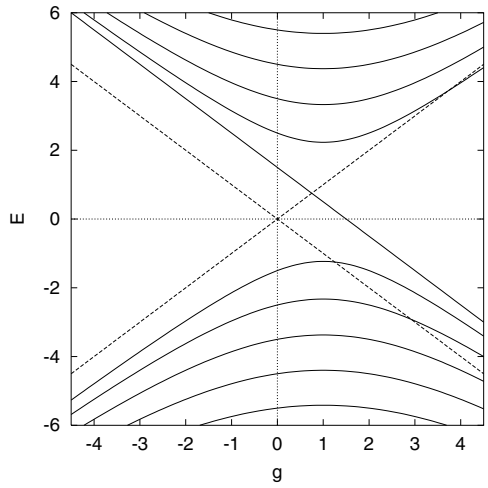

Figure 2. The energy levels E_n as a function of the coupling constant g for $f(\mu) = \mu$. $E = \pm g$ is shown as dashed lines.

with energy E_0 is only symmetric under combined reflections $g \to 2 - g$ and $E \to 1 - E$, which corresponds to a π-rotation around the point $\left(E = \frac{1}{2}, g = 1\right)$. This spectrum agrees with our previous calculation where we used the fact that $G(u)$ is an integral function.

5. Numerical results

In this section we first describe numerical algorithms to calculate the spectrum for more general shape functions $f(\mu)$. Then we discuss the spectrum for the conformal ansatz (2.22). We also discuss the simple ansatz $f(\mu) = B\mu$ which gives rise to skyrmions with $B > 1$. Finally, we compare our results with the literature.

5.1. Numerical algorithm

The energy spectrum can be calculated for various shape functions using a standard relaxation method [24]. The differential equation (3.21) is rewritten as a system of first order differential equations,

$$\begin{aligned} y_1{}'(u) &= y_2(u) \\ y_2{}'(u) &= h(y_1(u), y_2(u), E). \end{aligned} \tag{5.1}$$

The energy E is considered as an additional dependent variable whose derivative vanishes, $y_3(u) \equiv E$, so that the complete system becomes

$$\begin{aligned} y_1{}'(u) &= y_2(u) \\ y_2{}'(u) &= h(y_1(u), y_2(u), y_3(u)) \\ y_3{}'(u) &= 0. \end{aligned} \tag{5.2}$$

For simplicity, let us discuss the numerical algorithm for $O(4)$ symmetric shape function $f(\mu) = \mu$. Equation (4.24) has a regular singular point at $u = -1$ which implies that at this point we cannot choose value and derivative of the solution independently. However, once the

value of $G(-1)$ is chosen, we can calculate $G'(u) = \frac{\mathrm{d}}{\mathrm{d}u}G(u)$. In fact, inserting $u = -1$ into equation (4.24), we obtain

$$G'(-1) = -\tfrac{1}{3}\big(E^2 - g^2 + 3g - \tfrac{9}{4}\big)G(-1). \tag{5.3}$$

Similarly we obtain for $u = 1$,

$$G'(1) = \frac{1}{5}\left(E^2 - g^2 + g - \frac{9}{4} + \frac{3g}{E+g}\right)G(1). \tag{5.4}$$

The system (5.2) is discretized such that the boundary conditions at the singular points $u = \pm 1$ are satisfied. Starting from an initial configuration, the relaxation algorithm calculates an improved configuration by linearizing the equation around the solution and minimizing an error function which indicates how well the discretized equations are satisfied.

The secret of a successful relaxation method is a good guess for the starting configuration. Fortunately, for $g = 0$ the analytic solution of (3.21) is known for all possible shape functions $f(\mu)$. Therefore, we start with this configuration at $g = 0$ and increase g by a small amount δg. The relaxed solution is a good initial configuration for $2\delta g$, and so on.

As a test, the spectrum for $f(\mu) = 0$ is calculated using the relaxation method. This reproduces the analytic result. For $f(\mu) = \mu$ the relaxation method converges well as long as $-\frac{E}{g}$ is not inside the interval $[-1, 1]$. However, if the regular singular point $-\frac{E}{g}$ is inside the interval, the relaxation algorithm no longer converges and has to be modified. This is one of the main reasons for including the lines $E = \pm g$ in the figures.

In this case a specially chosen shooting method proves more suitable. It deals with the additional singularities in $[-1, 1]$ by simply avoiding them. As mentioned before, our differential equation can be defined on the complex plane. Due to the boundary condition, the solution $G(u)$ is an analytic function. The original solution is recovered by restricting $G(u)$ to be a real function of a real variable $u \in [-1, 1]$. In order to avoid further singular points on the real line, we can set $u = \exp(\mathrm{i}\phi)$ where $\phi \in [0, \pi]$. Then equation (3.21) induces a differential equation for ϕ, that is the equation is solved on a semicircular contour. The resulting differential equation can be written as a system of five real first order differential equations, one of which corresponds to the energy E. Now, the spectrum can be obtained by a standard shooting method [24]. The boundary conditions for the shooting method are that at the singular points $u = \pm 1$, the solution is non-singular and furthermore that the equation is real at $u = -1$. Since the equation has real coefficients, the fact that $G(u)$ is real for $u = -1$ implies that $G(u)$ is real for $u \in [-1, 1]$.

A successful shooting method needs a good initial guess. For $g = 0$ we can rely on our explicit solution and impose $G(-1) = 1$ and

$$G(1) = \frac{\Gamma\big(\frac{3}{2}\big)\Gamma\big(-\frac{3}{2}\big)}{\Gamma(e)\Gamma(-e)} \tag{5.5}$$

$$= -\tfrac{2}{3}e\sin(\pi e) \tag{5.6}$$

where equation (5.5) follows from equation (4.22) and equation (5.6) follows from the reflection relation for the gamma function (see (6.1.17) in [21]). As in the relaxation method, the initial guess for the coupling constant $g + \delta g$ is the value of the solution for coupling constant g.

It is also possible to reconstruct the solution $G(u)$ for $u \in [-1, 1]$ using the solution $G(\exp(\mathrm{i}\phi))$ for $\phi \in [0, \pi]$. Cauchy's formula states that if $f(z)$ is an analytic function and C is a contour enclosing the point a, then

$$f^{(n)}(a) = \frac{n!}{2\pi\mathrm{i}}\oint_C \frac{f(z)\,\mathrm{d}z}{(z-u)^{n+1}} \tag{5.7}$$

see for example [20, p 90]. In our case $G(u)$ is a real function on the interval $[-1, 1]$, so

$$G(u) = \sum_{k=0}^{\infty} a_k u^k \tag{5.8}$$

where the coefficients a_k are real. It follows that $G(u)$ can be written as

$$G(u) = \frac{1}{\pi} \operatorname{Re}\left(\int_0^{\pi} \frac{G(\mathrm{e}^{\mathrm{i}\phi})\, \mathrm{e}^{\mathrm{i}\phi}\, \mathrm{d}\phi}{\mathrm{e}^{\mathrm{i}\phi} - u} \right) \tag{5.9}$$

and a similar formula can be obtained for its derivative $G'(u)$. For $E^2 > g^2$ both the relaxation method and the shooting method give the same result.

5.2. Generalization to more complicated skyrmions

With the conformal shape function (2.22), equation (3.21) gives rise to a rather lengthy differential equation with five regular singular points, see [25] for more details. Assuming that the singular points do not coalesce, we obtain the following exponents:

$$\begin{aligned}
\rho_{1,2}^{(1)} &= \left(0, -\tfrac{3}{2}\right) \\
\rho_{1,2}^{(-1)} &= \left(0, -\tfrac{1}{2}\right) \\
\rho_{1,2}^{(\frac{Ea-gb}{Eb-ga})} &= (2, 0) \\
\rho_{1,2}^{(\frac{a}{b})} &= (0, 0) \\
\rho_{1,2}^{(\infty)} &= \left(\tfrac{3}{2} \pm \sqrt{E^2 - g^2}\right)
\end{aligned} \tag{5.10}$$

where $a = k^2 + 1$ and $b = k^2 - 1$ and $k > 1$. The relation (4.15) is again satisfied. Moreover, the exponents at infinity are the same as for $f(\mu) = 0$. In the limit $k \to 1$ the exponents at infinity change discontinuously (see (4.25)). The exponents change if one or more singular points coalesce. However, in general, there are five singular points which all have different characteristics.

The regular singular points at $u = \pm 1$ provide the boundary conditions for the regular solution, and are not very sensitive to the exact form of the shape function. They imply that the solution of this equation locally still is ananalytic function of u. One might expect that the regular singular point at infinity could be used to calculate the degree of the polynomial as in the previous two sections. However, for general k, the solutions are not regular on the entire complex plane, so that the exponents at infinity do not contain any information about the spectrum. This is because there is a further singular point at $u = \frac{b}{a}$ with exponents $(0, 0)$. Generically, the solution diverges logarithmically at this singular point such that $u = \frac{b}{a}$ is a branch point, see equation (4.14). The existence of polynomial solutions might be related to the spherical $O(4)$ symmetry of the problem, which is broken for $k \neq 1$. Note that the singular point at $\frac{a}{b} = \frac{k^2+1}{k^2-1}$ is independent of E, and it can never be inside the interval $(-1, 1)$ because $(k^2+1)^2 > (k^2-1)^2$ for $k \in (0, \infty)$. Finally, the singular point at $\frac{Ea-gb}{Eb-ga}$ depends on the energy E. Moreover, for certain values of E, k and g, this point can be inside the interval $(-1, 1)$. This singular point could force a potential solution to diverge, such that it would no longer be well defined. Therefore, we are interested in the local behaviour near $u = \frac{Ea-gb}{Eb-ga}$. After a straightforward but long calculation using Maple, we obtain $g_2 = 0$. Therefore, locally, both solutions are convergent power series, and no logarithmic divergencies occur.

In the following we calculate spectra as a function of the coupling constant g for different values of k numerically. For $k = 1$ we reproduce the spectrum for $f(\mu) = \mu$ of section 4.3.

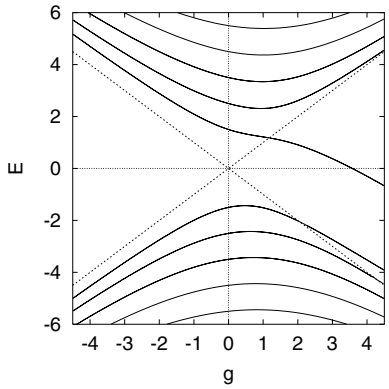

Figure 3. The spectrum using (2.22) for the shape function $f(\mu) = 2\arctan\left(k\tan\frac{\mu}{2}\right)$ where $k = 5$. $E = \pm g$ is shown as dashed lines.

Also note that $k = \infty$ corresponds to the spectrum for $f(\mu) = \pi$ which agrees with the spectrum for $f(\mu) = 0$ in section 4.2. As k increases, the spectrum moves towards the $k = \infty$ spectrum. At the same time, the energy E_0 intersects $E = 0$ for increasing values of the coupling constant g, such that for $k \to \infty$ the intersection point also appears to move to ∞. In figure 3 we display the spectrum for $k = 5$.

In the following we discuss the eigenfunction which crosses zero in more detail. We restrict out attention to the following Lorentz scalar Q which is defined as

$$Q = \int_{S^3} \bar{\psi}\psi. \tag{5.11}$$

A short calculation shows that $\bar{\psi}\psi$ is a function of μ only. Therefore, we can integrate out the angular coordinates θ and ϕ and obtain:

$$Q = \int_0^\pi \tilde{Q}(\mu)\,\mathrm{d}\mu \tag{5.12}$$

$$= 4\pi \int_0^\pi ((1-\cos\mu)G^2 + (1+\cos\mu)\tilde{G}^2)\sin^2\mu\,\mathrm{d}\mu. \tag{5.13}$$

The density $\tilde{Q}(\mu)$ measures where the fermion field is localized. To obtain equation (5.13) we used equations (3.15) and (3.23). $G(u)$ and $\tilde{G}(u)$ can be calculated from (3.21) and (3.22), respectively. Recall $u = \cos\mu$. Expressing $F(u)$ in terms of $\tilde{G}(u)$ avoids having to worry about the denominator in (3.24) which is rather difficult to handle numerically. Note, however, that $F(u)$ is non-singular for $E + g\cos f = 0$. This follows from the behaviour at the corresponding regular singular point of equation (3.21). The function $\tilde{G}(u)$ is related to $G(u)$ via equations (3.23) and (3.24). This implies

$$\tilde{G}(1) = -\frac{3}{2(E+g)}. \tag{5.14}$$

In the following, we calculate $\tilde{Q}(\mu)$ for $k = 1, 2$ and 5 and compare it to the baryon density

$$\tilde{B}(\mu) = \frac{2}{\pi} f'(\mu)\sin^2 f(\mu). \tag{5.15}$$

which measures where the Skyrme field is localized[6].

[6] Usually, $\tilde{B}(\mu)$ is defined with a minus sign, but this is of no relevance here.

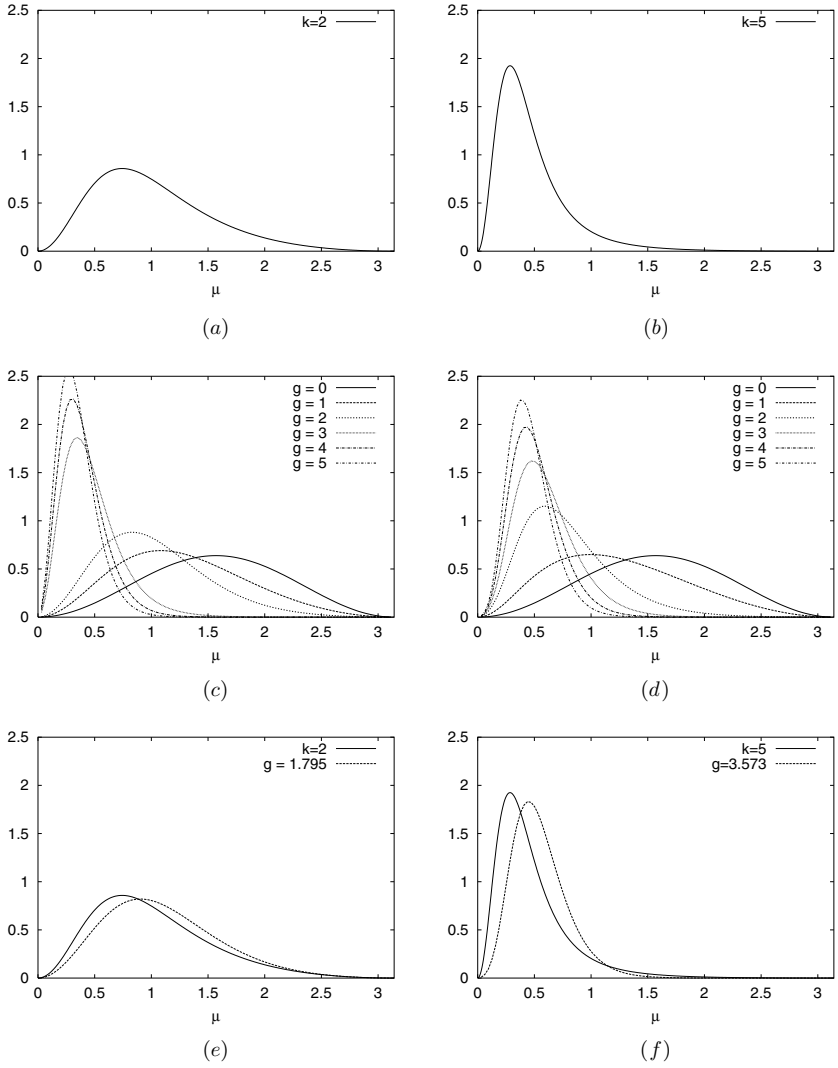

Figure 4. In this figure we display $\tilde{B}(\mu)$ and $\tilde{Q}(\mu)$ as a function of μ for $k = 2$ and 5, and for various values of the coupling constant g: (*a*) $\tilde{B}(\mu)$ for $k = 2$, (*b*) $\tilde{B}(\mu)$ for $k = 5$, (*c*) $\tilde{Q}(\mu)$ for $k = 2$ for $g = 1, 2, 3, 4, 5$, (*d*) $\tilde{Q}(\mu)$ for $k = 5$ for $g = 1, 2, 3, 4, 5$, (*e*) comparison of $\tilde{Q}(\mu)$ and $\tilde{B}(\mu)$ for $k = 2$ and (*f*) comparison of $\tilde{Q}(\mu)$ and $\tilde{B}(\mu)$ for $k = 5$.

The expression for ψ can be calculated explicitly for $k = 1$. In this case $G(u) = a_0$. Since we are interested in the zero crossing mode, we have to set $E = \frac{3}{2} - g$ and obtain

$$\tilde{Q}(\mu) = 8\pi a_0^2 \sin^2 \mu. \tag{5.16}$$

Surprisingly, this is independent of g. Also note that in this case $\tilde{Q}(\mu)$ is proportional to $\tilde{B}(\mu)$. In the following, we normalize $\tilde{Q}(\mu)$ so that $Q = 1$.

For $k > 1$, the Skyrme configuration is localized near the north pole $\mu = 0$ (see figure 4). In figures 4(*a*) and (*b*) we show $\tilde{B}(\mu)$ for $k = 2$ and $k = 5$, respectively. In figures 4(*c*) and (*d*) we show $\tilde{Q}(\mu)$ for several values of the coupling constant g. For $g = 0$, $\tilde{Q}(\mu)$ can also be calculated explicitly and is independent of k. For $k > 1$ and $g > 0$,

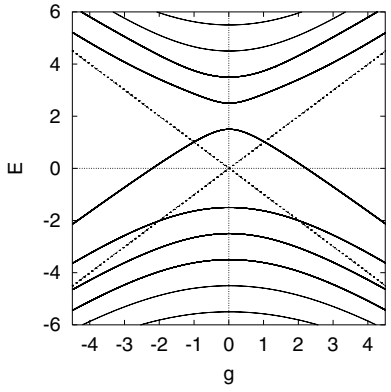

Figure 5. The spectrum using $f(\mu) = 2\mu$. $E = \pm g$ is shown as dashed lines.

the fermion configuration is also localized near the north pole. For $k = 2$, the energy E vanishes when $g \approx 1.795$. For $k = 5$, the energy E vanishes when $g \approx 3.573$. In figures 4(e) and (f) we display $\tilde{Q}(\mu)$ for these values of g and compare it to the baryon density $\tilde{B}(\mu)$. There is quite a good agreement between these two functions. Therefore, the $E = 0$ states can be interpreted as a fermion–skyrmion bound states.

The simplest method for obtaining a skyrmion with baryon number $B > 1$ is the ansatz $f(\mu) = B\mu$. For $B > 1$ this Skyrme configuration has very high energy. However, we are mainly interested in the interplay of topology and the spectrum of the Dirac equation which should be independent of the precise form of the skyrmion.

For $B = 2$ the spectrum is displayed in figure 5. It is symmetric with respect to the E-axis. Note that the symmetry of the spectrum can be derived from equations (3.21) and (3.22). For even B the function $\cos f$ is an even function of u, and $\sin f$ is an odd function of u. Under $g \to -g$ and $u \to -u$, equations (3.21) transforms into equation (3.22). However, the equations are just expressed in different coordinate systems, and hence have the same energy eigenvalues. Therefore, we have shown that the spectrum is symmetric under $g \to -g$ if B is even, provided that f is an odd function of u.

For $g = 0$ all the eigenmodes have the same value, independent of the background configuration and parity. As g increases, the modes increasingly feel the influence of the background configuration, in particular its topology. It appears that the winding number $B = 2$ of the skyrmion forces two modes to cross zero, one for $g > 0$ and one for $g < 0$. In order to follow the spectrum for $E^2 < g^2$, the shooting method has to be used.

This pattern can also be verified for $B = 3$, see figure 6. Now there are three modes which cross zero, two of positive parity ($g > 0$) and one of negative parity ($g < 0$). It seems probable that the number of zero-crossing modes of positive parity differs at most by one from the number of zero-crossing modes of negative parity. Further calculations for $B = 4$ and 5 confirm this pattern. For $B = 4$ we find two zero-crossing modes of positive parity and two of negative parity, whereas for $B = 5$ there are three positive parity modes and two negative parity modes.

This numerical evidence shows that the singular points of equation (3.21) play an important role. In the following we will assume that $f(\mu)$ is an analytic function, and in particular that it can be expanded in a Taylor series with respect to the variable $u = \cos\mu$, for $u \in (-1, 1)$. It follows that $\cos f$ and $\sin f$ are also analytic functions of u. Therefore, the only singular points of (3.21) inside the interval $(-1, 1)$ occur for $\cos f = -E/g$. If such a singular point

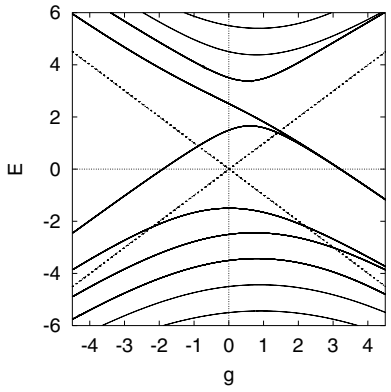

Figure 6. The spectrum using $f(\mu) = 3\mu$. $E = \pm g$ is shown as dashed lines.

is non-degenerate, its exponents are 0 and 2. Furthermore, it can be shown by expanding f as a power series in u that the coefficient g_2 always vanishes. In our previous examples $f(\mu)$ was always monotonic. Let $f(\mu)$ be monotonic with boundary conditions $f(0) = 0$ and $f(\pi) = B\pi$. If $E^2 < g^2$, then $\cos f = -E/g$ has B non-degenerate solutions for $u_i \in (-1, 1)$. In this case, these singularities of equation (3.21) all have exponents $(2, 0)$ and the coefficient g_2 vanishes, so that the solution of (3.21) is regular at these points. We conjecture that the existence of B regular singular points inside the interval $(-1, 1)$ indicates that there are B modes crossing from one side of the spectrum to the other. This conjecture is equivalent to the statement that for topological charge B there are B modes that cross zero[7].

If we allow for more general Skyrme configurations than the hedgehog, such a statement becomes even more difficult to prove, because now we have to solve partial differential equations. However, both the topological number and the number of singular points are stable under small perturbations. Therefore, there seems to be a deep interplay between the topology of the configuration and the singular points of a differential operator. This can be compared to monopoles where we have an index theorem which connects the topology of the monopole configuration with the index of the Dirac operator.

In the following we compare our results with the literature. Kahana and Ripka considered the problem of coupling a hedgehog configuration to fermions in flat space using an approximation for the Skyrme configuration with a size parameter. Varying this parameter they computed the spectral flow of the eigenvalues. They found a 0^+ zero mode for a special value of the 'size' of the hedgehog. Since the size is given by minimizing the energy density for the skyrmion, their result corresponds to varying the coupling constant g.

In [10] a linear approximation for the shape function, $f(r) = \pi\left(1 - \frac{x}{X}\right)$, was used. Here $x = g \cdot r$ so that the Dirac equation for the fermions is independent of g. However, we defined the skyrmion as a given background configuration which minimizes the energy. Therefore, $X = g \cdot R_{\mathrm{Sk}}$ where R_{Sk} is the size of the skyrmion. R_{Sk} can be calculated by minimizing the energy [26]: $R_{\mathrm{Sk}} = 1.67$. Kahana and Ripka showed by numerical calculation that there is a zero mode for $X = 3.2$ which corresponds to $g = 1.9$. In [12] an exponential function was used to approximate the shape function: $f(r) = \pi \exp\left(-\frac{x}{X}\right)$. In this case minimizing the energy results in $R_{\mathrm{Sk}} = 1.7$ and the zero mode occurs for $X = 2$ which corresponds to

[7] The existence of such zero-crossing modes has also been discussed recently by Balachandran *et al* in a more geometric language. The authors discovered a relation between these modes and Euclidean instantons.

$g = 1.1$. The fact that there is a mode which crosses zero seems to be independent of the special ansatz for the shape function. This is consistent with our results.

In [17] it has been argued that a skyrmion in flat space is reasonably well approximated by the stereographic projection of a skyrmion on a 3-sphere of optimal radius. The optimal radius for $B = 1$ is $L = 1$ so we can use our analytic result for the mode E_0 in section 4.3. For $g = \frac{3}{2}$ this is a zero mode, and the value of g is in the same order of magnitude as in the literature mentioned above.

6. Conclusion

We have derived the Dirac equation for fermions on the 3-sphere which are chirally coupled to a skyrmion. In this paper, we only considered spherically symmetric Skyrme configurations and fermionic states with the total angular momentum $G = 0$. We were particularly interested in the shape functions $f(\mu) = 0$ and $f(\mu) = \mu$ and the conformal ansatz (2.22).

The shape function $f(\mu) = 0$ leads to a hypergeometric equation and can therefore be solved explicitly in terms of hypergeometric functions. To derive the spectrum we have to impose that the solutions are non-singular at the north and south poles using the correct chart. We derived the spectrum

$$E = \pm\sqrt{g^2 + \left(N + \tfrac{3}{2}\right)^2} \qquad \text{for} \quad N = 0, 1, 2, \ldots$$

which agrees with the spectrum calculated by Sen [22] using Maurer Cartan forms. Moreover, the eigenfunctions $G_N(u)$ are given by Jacobi polynomials.

The shape function $f(\mu) = \mu$ is more complicated. It leads to a Fuchsian equation with four regular singular points, two at the boundary $u = \pm 1$, one at infinity and one depending on E and g. However, the equation could still be solved in terms of polynomials. We were able to solve the recurrence relation for the coefficients of the polynomial and derived the corresponding spectrum:

$$E_0 = \tfrac{3}{2} - g$$

$$E_n^{\pm} = \tfrac{1}{2} \pm \sqrt{n^2 + 2n + (g-1)^2} \qquad \text{for} \quad n = 1, 2, \ldots.$$

The eigenfunctions have been evaluated explicitly:

$$G_0(u) = a_0$$

$$G_n(u) = \sum_{k=0}^{n} a_k \, (u+1)^k$$

where

$$a_k = \frac{\left(E + g - \frac{3}{2}\right)\left(E + g - \frac{k}{2}\right)}{k!(2k+1)!!} \prod_{i=1}^{k} \left(E^2 - E + 2g - g^2 + \frac{1}{4} - (\mathrm{i}+1)^2 \right).$$

We also considered more general shape functions numerically. For $B = 1$ we discussed the conformal ansatz (2.22) and calculated the spectrum. For $k = 1$ the spectrum agrees with the analytic solution. In particular there is a mode 0 whose energy E_0 crosses zero for a certain value of the coupling g. The graph of E_0 as a function of g changes as the parameter k in the ansatz is varied. However, for finite $k > 0$, this mode always stays present. According to our numerical evidence, the eigenfunction for $E = 0$ can be interpreted as a fermion–skyrmion bound state.

For larger B we considered the ansatz $f(\mu) = B\mu$. This leads to B modes crossing zero. We conjectured a connection between zero modes and certain singular points in the equation which in turn are connected to the winding number of the configuration.

Acknowledgments

The author wants to thank N S Manton, H Pfeiffer and Y Shnir for many discussions during various stages of this project. The author also would like to thank J M Speight for many helpful suggestions and continuous support.

References

[1] Skyrme T H R 1961 A nonlinear field theory *Proc. R. Soc.* A **260** 127
[2] Adkins G S, Nappi C R and Witten E 1983 Static properties of nucleons in the Skyrme model *Nucl. Phys.* B **228** 552
[3] Leese R A, Manton N S and Schroers B J 1995 Attractive channel skyrmions and the deuteron *Nucl. Phys.* B **442** 228 (*Preprint* hep-ph/9502405)
[4] Irwin P 2000 Zero mode quantization of multi-skyrmions *Phys. Rev.* D **61** 114024 (*Preprint* hep-th/9804142)
[5] Krusch S 2003 Homotopy of rational maps and the quantization of skyrmions *Ann. Phys., NY* **304** 103 (*Preprint* hep-th/0210310)
[6] Finkelstein D and Rubinstein J 1968 Connection between spin, statistics, and kinks *J. Math. Phys.* **9** 1762
[7] Witten E 1983 Global aspects of current algebra *Nucl. Phys.* B **223** 422
[8] Balachandran A P and Vaidya S 1999 Skyrmions, spectral flow and parity doubles *Int. J. Mod. Phys.* A **14** 445 (*Preprint* hep-th/9803125)
[9] Hiller J R and Jordan T F 1986 Solutions of the Dirac equation for fermions in Skyrme fields *Phys. Rev.* D **34** 1176
[10] Kahana S and Ripka G 1984 Baryon density of quarks coupled to a chiral field *Nucl. Phys.* A **429** 462
[11] Ripka G and Kahana S 1985 The stability of a chiral soliton in the fermion one loop approximation *Phys. Lett.* B **155** 327
[12] Ripka G 1997 *Quarks Bound by Chiral Fields* (Oxford: Oxford Science Publications)
[13] Manton N S and Ruback P J 1986 Skyrmions in flat space and curved space *Phys. Lett.* B **181** 137
[14] Manton N S and Schroers B J 1993 Bundles over moduli spaces and the quantization of BPS monopoles *Ann. Phys., NY* **225** 290
[15] Nakahara M 1990 *Geometry, Topology and Physics (Graduate Student Series in Physics)* (Bristol: Institute of Physics Publishing)
[16] Eguchi T, Gilkey P B and Hanson A J 1980 Gravitation, gauge theories and differential geometry *Phys. Rep.* **66** 213
[17] Krusch S 2000 S^3 skyrmions and the rational map ansatz *Nonlinearity* **13** 2163 (*Preprint* hep-th/0006147)
[18] Gell-Mann M and Levy M 1960 The axial vector current in beta decay *Nuovo Cimento* **16** 705
[19] Manton N S 1987 Geometry of skyrmions *Commun. Math. Phys.* **111** 469
[20] Whittaker E T and Watson G N 1927 *A Course of Modern Analysis* 4th edn (Cambridge: Cambridge University Press)
[21] Abramowitz M and Stegun I A 1972 *Handbook of Mathematical Functions* 10th edn (New York: Dover)
[22] Sen D 1986 Fermions in the space-time $R \times S^3$ *J. Math. Phys.* **27** 472
[23] Carmeli M and Malin S 1985 Field theory on $R \times S^3$ topology 3. The Dirac equation *Found. Phys.* **15** 1019
[24] Press W H, Flannery B P, Teukolsky S A and Vetterling W T 1992 *Numerical Recipes* (Cambridge, MA: Cambridge University Press)
[25] Krusch S 2001 Structure of skyrmions *PhD Thesis* University of Cambridge
[26] Adkins G S 1987 Static properties of skyrmions *Chiral Solitons* ed K Liu (Singapore: World Scientific)